計測自動制御学会産業論文集
Vol.6, No.10, 78/84 (2007)

Development and Assessment of GPS Precise Point Positioning Software for Land Vehicular Navigation

Masatoshi HONDA*, Masaaki MURATA* and Yukio MIZUKURA*

GPS precise point positioning (PPP) has attracted precision GPS community as it can provide the accuracy at the centimeter-decimeter level, which is almost comparable to that obtained by kinematic GPS. In this paper we have originally developed a PPP software for vehicular navigation applications, in that models are pursued so as to be consistent to those used in the IGS precise ephemeris generation. Assuming pseudorange and carrier phase data from a single dual-frequency receiver and using IGS precise satellite ephemeris and clock information, the software estimates a position vector of a moving (and static) antenna, a clock bias of the user receiver, tropospheric delay parameters, and ionospheric-free (float) ambiguities in the undifferenced carrier phase data. In particular, all unknowns are assumed to be random walk processes. Our PPP filter design approach with software has been validated by using a series of GPS experiment data for static and moving antennas and analyzing data in post-processing mode. The results have shown that the developed software could yield a 2D accuracy of a few centimeters for static mode and at a decimeter level for kinematic mode, also reconfirming the reported superior performance of PPP for land vehicular navigation.

Key words: GPS, precise point positioning, IGS, precise orbit and clock, EKF

1. Introduction

Recently, GPS precise point positioning (PPP) has attracted precision GPS community as the centimetr-decimeter accurate positioning results have been demonstrated [1),2),3)]. Such a PPP technique has become possible with the availability of precise orbits and clock correction information for the GPS satellites from IGS (International GNSS service)[4)]. This accuracy level is almost comparable to that obtainable with carrier phase DGPS, i.e. kinematic GPS[3)]. While DGPS requires at least two receivers and radio link between them, and its use is limited generally in the range of about 20 km in baseline length, PPP can work anywhere with a single GPS receiver only, thus yielding significant operational flexibility and cost reduction.

Therefore PPP will be an alternative to the conventional DGPS, and it would find wide areas of application such as remote sensing, monitoring natural hazards, vehicular navigation, etc. The application to precision autonomous navigation for unmanned aerial or land vehicles is especially interesting.

* Department of Aerospace Engineering, National Defense Academy, HASHIRIMIZU 1-10-20, YOKOSUKA, KANAGAWA-PREF. 239-8686, JAPAN
(Received March 23, 2007)

We have originally developed a PPP software for vehicular navigation applications as well as static control survey, which uses both pseudorange and carrier phase data from a single dual frequency receiver and IGS products. In this paper we present the feature of the developed software and its validation results by processing, in post-mission mode, the GPS experiment data acquired under static and moving antenna environments.

2. PPP Filter Design and Software Development

Implicitly assumed is that the receiver is two-frequency so that ionospheric-free pseudorange and carrier phase data are available. In that case the observation equations are written in the form of the linear combination:

$$PR = \frac{f_1^2 \cdot PR_1 - f_2^2 \cdot PR_2}{f_1^2 - f_2^2} = \rho + cdt + d_{trop} + \varepsilon_{PR}$$

$$\Phi = \frac{f_1^2 \cdot \Phi_1 - f_2^2 \cdot \Phi_2}{f_1^2 - f_2^2} = \rho + cdt + d_{trop} + \tilde{N} + \varepsilon_{\Phi}$$

$$\tilde{N} = \frac{cf_1^2 \cdot N_1 - cf_2^2 \cdot N_2}{f_1^2 - f_2^2}$$

where PR_i is the measured pseudorange on L_i; Φ_i is the measured carrier phase on L_i; ρ is the true geometric range; c is the speed of light; dt is the receiver clock bias; d_{trop} is the tropospheric delay; f_i is

the frequency of L_i; N_i is the integer phase ambiguity on L_i; ε is the measurement noise.

The total troposheric delay is modeled [5] by

$$d_{trop} = H_{dry} m_{dry}(e) + H_{wet} m_{wet}(e) + [G_{north} \cos(a) + G_{east} \sin(a)] m_{gradient}(e)$$

where H_{dry}, H_{wet} are the zenith hydrostatic delay and zenith wet delay; G_{north}, G_{east} are the horizontal delay gradients in the north and east directions; $m_{dry}(e)$ is the hydrostatic mapping function; $m_{wet}(e)$ is the wet mapping function; a, e are the azimuth and elevation angles. The zenith hydrostatic delay can be predicted with high fidelity by the Saastamoinen model, which can be described [6] by

$$H_{dry} = \frac{0.0022768\, P_0}{1 - 0.00266 \cos 2\varphi - 0.00028\, H}$$

where P_0 is the barometric pressure in millibars, φ is the latitude and H is the geodetic height in killometers. For the mapping functions $m_{dry}(e)$ and $m_{wet}(e)$, we have selected the Niell's mapping functions (NMF)[7] because of higher accuracy and precision, and because no surface meteorology is necessary for its implementation. For the gradient mapping function $m_{gradient}(e)$,

$$m_{gradient}(e) = \frac{1}{\sin(e)\tan(e) + 0.0032}$$

is implemented [8].

The zenith hydrostatic delay H_{dry} can be either fixed or estimated, and the other parameters H_{wet}, G_{north}, and G_{east} are the solve-for parameters to be estimated simultaneously with other unknowns.

Navigation or positioning user can use the precise orbits and clocks produced by IGS. The IGS's official products for precise orbits and clocks are in three categories: UltraRapid, Rapid, and Final [4]. Among these products, only the UltraRapid orbit and clock can be used in real-time. However, in this analysis we have used the Rapid orbit and clock products. The Rapid products of precise orbits and clocks are offered at 15-minute and 5-minute intervals, respectively. Computing satellite position/velocity and clock corrections at the epochs of data is performed by using Lagrange's polynomial interpolation of 9th order for orbits and of 2nd order for clock corrections.

Among phenomena causing site displacements, only solid earth tide is modeled [9] in the current version, and the correction for the center-of-mass offset of the transmitting antenna is applied. For doing these corrections the planetary ephemerides for the Sun and the Moon are required, to which two options are available in the software, accurate ephemeris by using JPL ephemeris tape (DE200) and less accurate one by analytical orbital theory. Also, relativistic corrections[1] are all taken into account.

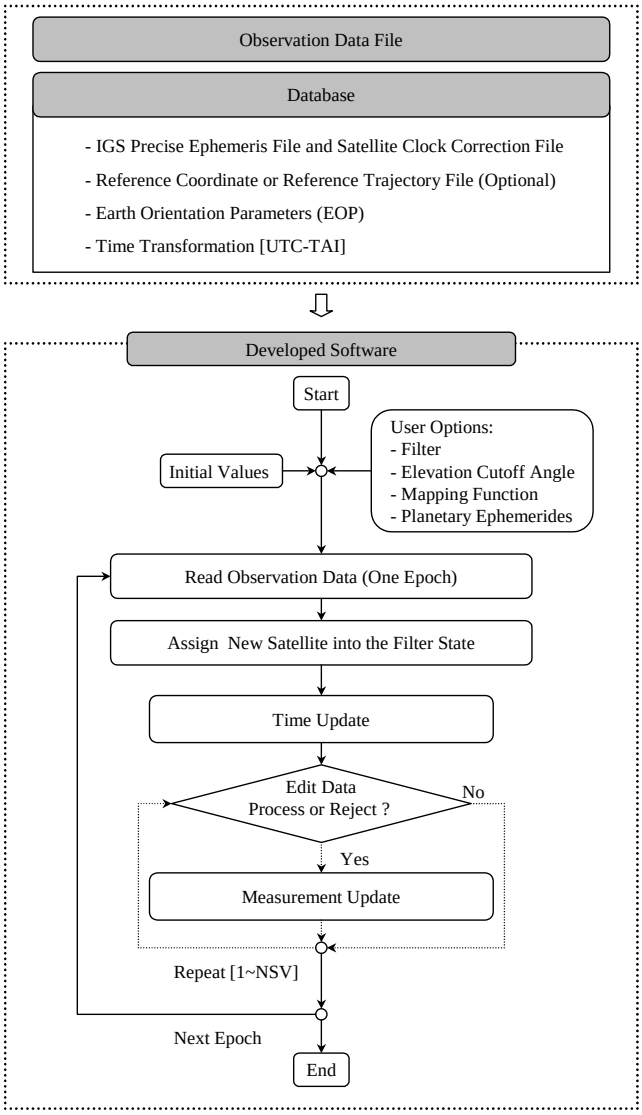

Fig.1 Structure and flowchart of the developed PPP software using a sequential estimation algorithm

The solve-for parameters are position components (3) of the receiver antenna, a receiver clock bias (1), tropospheric delay parameters (4), and ionospheric-free (float) ambiguities (12) in the undifferenced carrier phase data. The maximum number of unknown ambiguities is fixed with the number of receiver's channels (12 as usual), and an ambiguity of a newly coming up satellite can be automatically incorporated into the filter state. All unknowns are modeled as random walks with mean zero and specified variances:

$$x_{i,j+1} = x_{i,j} + w_{i,j}$$

where $w_{i,j} \sim N(0, Q_j(t_{j+1} - t_j))$. The $x_{i,j}$ denotes the i -th component of the state vector at t_j where

$$x = (r^T \; b \; H_{dry} \; H_{wet} \; G_{north} \; G_{east} \; \tilde{N}_1 \cdots \tilde{N}_{12})^T .$$

For parameter estimation, the Extended Kalman Filter (EKF) was implemented (see **Fig.1** for the structure and flowchart of the developed PPP software).

In particular, zenith wet delay is a random walk with a priori mean and standard deviation (STD) of zero and 10 cm, respectively, driven by white noise of $0.6 cm/\sqrt{h}$ STD. The tropospheric gradients are also modeled as random walks driven by white noises of $0.6 \; cm/\sqrt{h}$ STD. Each of the carrier phase float ambiguities has a 10 m a priori STD, and is treated as a random walk driven by 0.0006 $cm/\sqrt{h}$ white noise.

3. Numerical Results

The software validation along with PPP performance assessment has been conducted, in that three datasets, two static (Tsukuba and NDA) and one kinematic (Kashiwa), were analyzed in post-processing mode using nominally a full setup of models as described in the previous section, with elevation cutoff angle of 10 degrees, unless otherwise noted. In the analysis the average pressure calculated from the measured or reported barometric pressure record were applied to computing the a priori zenith hydrostatic delay, so that the estimated zenith wet delay and gradients would reflect the real residual tropospheric delay.

Tsukuba data

The first data to be analyzed are those observed on 22 November 2005 at 30-second interval by the Geographical Survey Institute (GSI) at Tsukuba, Ibaragi Pref. This is an IGS site. This dataset was available from the IGS data archives at the CDDIS of NASA Goddard Space Flight Center, and it covered the whole one day. No meteorological data have been reported from GSI. The receiver is an AOA (Allen Osborne Associates) benchmark ACT, and is driven by a cesium external oscillator. The precise coordinates for Tsukuba site on that day are also available from IGS Rapid products, which can be used as the "truth."

The 24-hour data on the day were processed by the EKF and the position solution was compared with the truth. The temporal behaviors of the positioning errors from the truth are shown in **Fig. 2**, and the corresponding accuracy statistics is tabulated in **Table 1**. Here, the dE, dN, and dU denote the positional error components expressed in the local east-north-up (ENU) frame. From Fig. 2, it is seen that the filter takes about 3 hours or even longer for convergence, so that we have excluded the first 3 hours of errors in calculating statistics in Table 1. After the convergence, the horizontal components are accurate at a few centimeters; the vertical component is less accurate at a sub-decimeter level; and the 3-D RMS error is 7 cm.

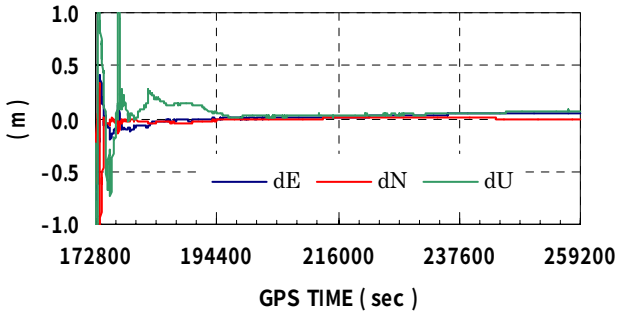

Fig. 2 Time history of the position errors (Tsukuba)

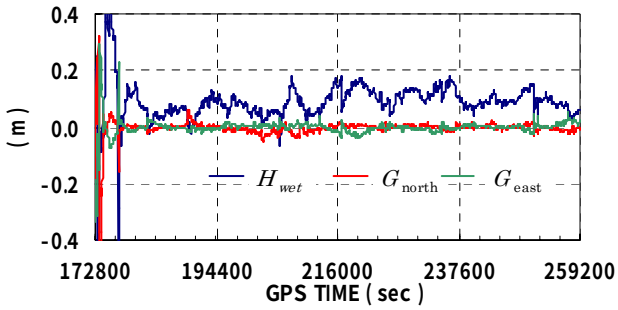

Fig. 3 Time history of tropospheric delay parameters

The results for the tropospheric parameter estimation are plotted in **Fig. 3**. We observe that the zenith wet delay is significantly time-varying, with mean (STD) of 9 cm (4 cm), and also that the mean values (STD) for the gradients $G_{north,}$ and G_{east} are -0.3 cm (1.2cm), -0.1 cm (1.1cm), respectively. Although no water vapor radiometer (WVR) data are available with Tsukuba data, the tropospheric wet delay inferred from these estimates should be highly correlated with WVR data on that day at the site.

The difference from the IGS Rapid very precise clock corrections for Tsukuba is plotted in **Fig. 4**. The

RMS and the mean (STD) are 0.57 and 0.43 (0.37), in nanoseconds, indicating the good coincidence within sub-nanosecond level.

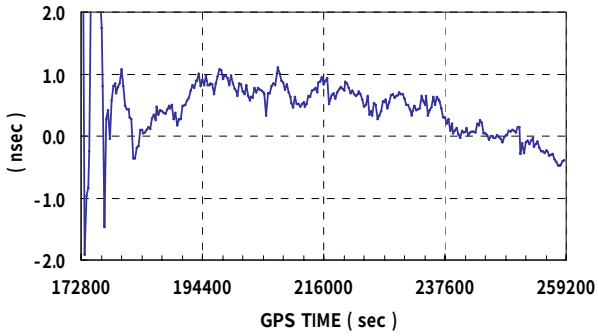

Fig. 4 Time history of the clock bias error

Table 1 Static positioning accuracy (Tsukuba)

	dE	dN	dU	3 D
RMS(m)	0.03	0.02	0.06	0.07
Mean(m)	0.02	-0.01	0.05	
STD(m)	0.02	0.01	0.04	

NDA data

On 22 November 2005, the static data were collected by using a dual- frequency GPS receiver (Novatel's OEM4) and an antenna with a ground plane for 6 hours at one second interval on the roof of the building at NDA, Yokosuka, Kanagawa Pref. Six hours of NDA full-rate data were analyzed by the developed software using the EKF assuming the same nominal setup as in the previous case. In order to obtain the reference coordinates or 'truth' of the antenna phase center, to which the PPP solution was compared, this dataset was submitted to the AUSLIG Online GPS Processing Service (so-called AUSPOS) operated by the National Mapping Agency, Australia. The positional errors from the truth is plotted in **Fig. 5**. The position accuracy is given in **Table 2**, where the statistics was calculated over 5 hours excluding the first one-hour period for the filter convergence. Again, we observe that: the horizontal error components, east and north direction, are accurate at the level of a few centimeters; the vertical error component is less accurate at a sub-decimeter level; and the 3-D RMS error is 9 cm. Although not shown here for the sake of economy, the mean values (STD) for H_{wet}, G_{north} and G_{east} were 1 cm (6cm), -0.03 cm (0.7cm), and -0.3 cm (0.9cm), respectively.

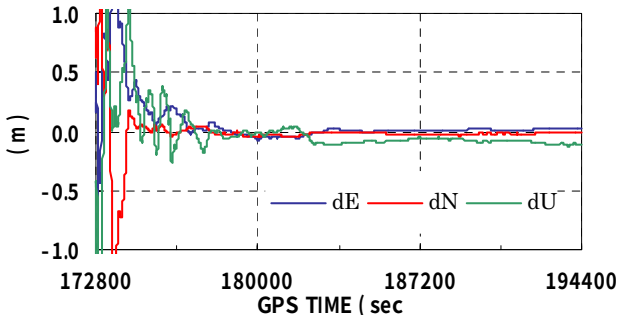

Fig. 5 Time history of the position errors (NDA)

Table 2 Static position accuracy (NDA)

	dE	dN	dU	3 D
RMS(m)	0.03	0.02	0.08	0.09
Mean(m)	0.01	-0.02	-0.06	
STD(m)	0.03	0.02	0.05	

Kashiwa data

On 7 June 2006, we conducted a GPS experiment for a moving antenna. A van was driven along a rural road in Kashiwa, Chiba Pref. Two GPS receivers, both Novatel's two-frequency OEM4s, participated in the experiment, one on the vehicle and another at a fixed location, to collect the observation data at the rate of one second. The vehicle's trajectory and the corresponding time record of the magnitude of the vehicle velocity vector, which were derived using a commercial kinematic GPS analysis software, are shown in **Figs. 6** and **7**.

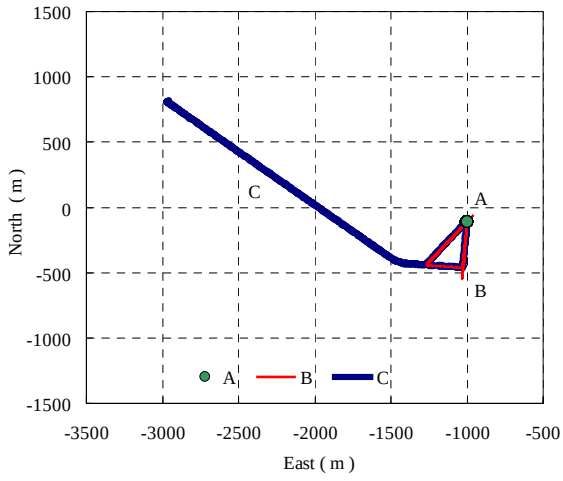

Fig. 6 Trajectory of the vehicle

As guessed from both figures the vehicle repeated configured runs, including frequent go-and-back, and with the longest straight run of 1.5 km. The total of 4-hour data was collected; in particular one hour at point A in static mode; and immediately then the

vehicle began driving to collect data for 3 hours in kinematic mode on the way of routes B and C. Note the average vehicle velocity of 5 m/s (for 2 hours) and 10 m/s (for 1 hour) over each route. The road is two-sided, and usually very few cars are running. The view along the route is mostly open to the sky.

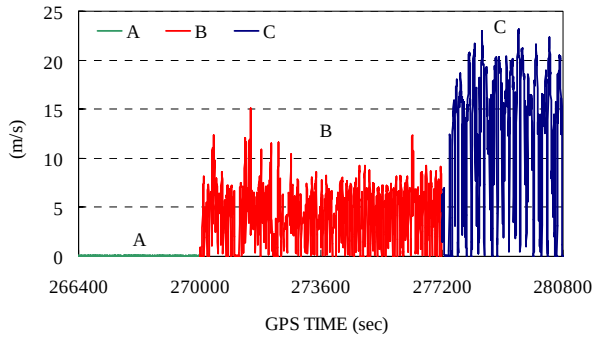

Fig. 7 Time history of the vehicle velocity

The distance between the fixed site and the vehicle was never more than about 3 km from each other. So, it was possible to resolve the phase ambiguities in L1 and L2, obtaining the very precise, L1-only, kinematic solution. This analysis was conducted by using a kinematic software called KINGS [10]. The resulting trajectory was used as the ground truth, to which the post-processing point positioning solutions were assessed.

The four hours of data were analyzed with 10-degree cutoff elevation angle, except for the decreasing white noises of 0.06 $cm/\sqrt{h}$ STD for the H_{wet} and gradients. In addition, another run was attempted to investigate the effect on the positioning accuracy of the changing cutoff angles: 5-degrees and 15-degrees. The number of lower-elevation-angle satellites versus the total number of visible satellites are shown in **Fig. 8**.

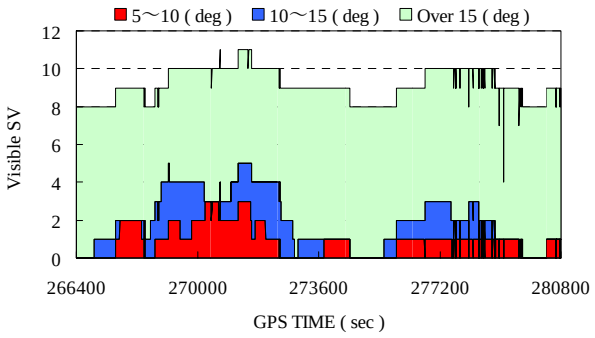

Fig. 8 The number of satellites in view

The position errors in the local ENU frame with the origin fixed at the reference site (base station) are shown in **Fig. 9**, in which three cases of 5-, 10-, and 15-degree cutoff angles are plotted, and the positioning accuracy for individual cutoff is given in **Table 3**, where the statistics was developed over the period of last 2 hours because of the filter convergence.

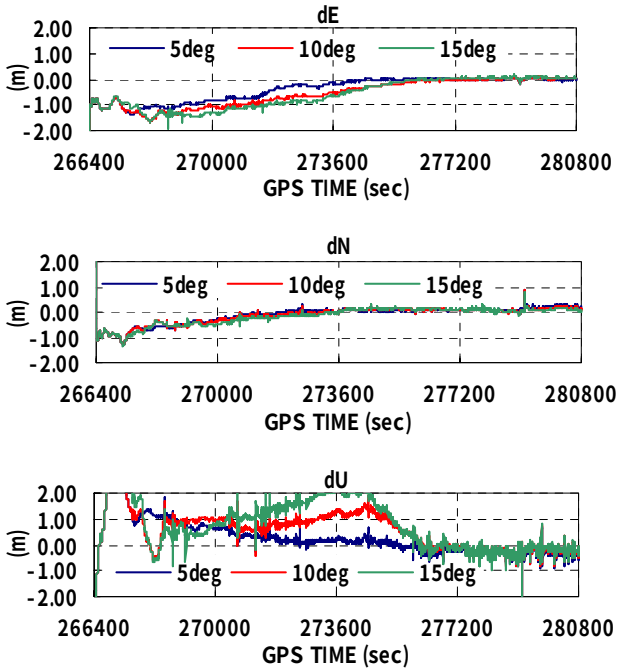

Fig. 9 Time history of the position errors (Kashiwa)

Table 3 Kinematic position accuracy (Kashiwa)

	cutoff angle	dE	dN	dU	3 D
RMS(m)	5(deg)	0.05	0.14	0.28	0.32
	10(deg)	0.19	0.12	0.65	0.69
	15(deg)	0.21	0.12	0.92	0.96
Mean(m)	5(deg)	-0.01	0.11	-0.17	
	10(deg)	-0.10	0.11	0.21	
	15(deg)	-0.07	0.10	0.36	
STD(m)	5(deg)	0.05	0.08	0.23	
	10(deg)	0.16	0.05	0.61	
	15(deg)	0.20	0.05	0.85	

The filter convergence seems to be much slow, taking 2-3 hours. Lowering cutoff angles have improved the positioning accuracy overall but not the convergence characteristics which have not changed so much. After convergence the positioning accuracy seems to be at the almost equal level for three cases of cutoff angles, being about a decimeter (RMS) horizontally, and a few decimeters (RMS) vertically. Note that accuracy figures clearly depend on the convergence definition. Since the convergence time is critical not only for

real-time navigation but also for static survey in a short session, methods for speeding up the convergence have to be pursued. Among them the proper setting for the magnitude of Q-matrix, use of a low cutoff angle with NMF, and the accurate initial a priori estimate of the state may be significant. The higher horizontal accuracy with PPP is especially promising for vehicular navigation on land. Moreover, the level of accuracy achieved in this study can be considered as the worst and does not always imply the potential performance of the PPP, because of the unordinary trajectory of the vehicle (see Fig. 6), to which the PPP was tested.

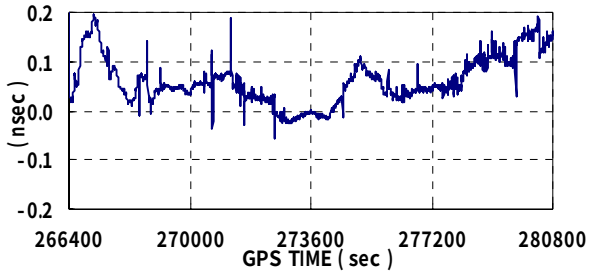

Fig. 10 Time history of the clock bias estimate

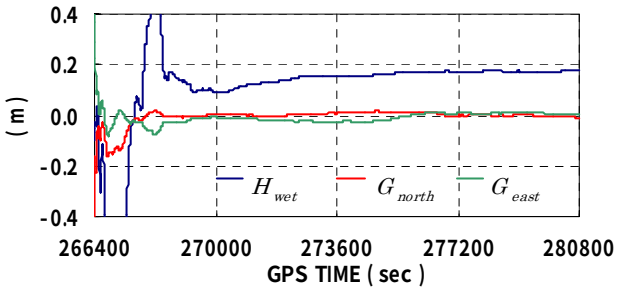

Fig. 11 Time history of tropospheric delay parameters

For reference the estimates for clock bias and tropospheric delay parameters are shown in **Figs. 10** to **11**. The estimated H_{wet} and gradients are, on average, about 20 cm and a few millimeters, respectively. On the contrary to the static case, reliable estimation of these nuisance parameters in kinematic mode is very much difficult, and so estimating only the zenith wet delay while navigating is of special concern. Several runs changing estimation strategy and cutoff angle were tried, and it turned out that the best result in terms of positioning quality and convergence property was with estimating H_{wet} and gradients and with 5-degree cutoff, following H_{wet} -only estimation with 10-degree cutoff. This may not be the whole story, but we need further evaluation using different sets of kinematic and longer data.

4. Concluding Remarks

We have developed and evaluated a basic PPP software workable in both static and kinematic modes, and reconfirmed the PPP performance using several GPS datasets. The main conclusions can be summarized as follows.

(1) Our software can achieve the point positioning accuracy at a few centimeter level in static mode, and at ten-odd centimeter level in kinematic mode, horizontally; and at sub-decimeter level in static mode and at the level of better than two decimeters in kinematic mode, vertically. These results clearly exhibit the validity of our design approach of the PPP filter and the developed software.

(2) The centimeter-decimeter accuracy of the PPP results can be achieved by estimating troposheric delay parameters and by possibly allowing lower elevation cutoff angle, and after the filter reaches the steady state. However, the filter generally converges much slowly, taking several tens minutes to a few hours depending on antenna's motion and environment, and so strategies for speeding up the convergence will be a future area of research.

Acknowledgements

We wish to thank all those who have provided information or helped during our research. Among them: Dr. T. Tsujii of JAXA for computing the Kashiwa double-differencing solutions by his program KINGS, Dr. H. Sugawara of NDA for supplying the meteorological data, and Dr. H. Namie of NDA for providing GPS receivers used in the GPS experiments.

[References]

1) J.Kouba and P.Heroux: Precise Point Positioning Using IGS Orbit and Clock Products, GPS Solutions, **5**-2, 12/28 (2001)

2) Y.Gao and K.Chen: Performance Analysis of Precise Point Positioning Using Real-Time Orbit and Clock Products, Journal of GPS, **3**-1/2, 95/100 (2004)

3) O.L.Colombo et al.: Evaluation of Precise, Kinematic GPS Point Positioning, Proc. of ION GNSS-2004 Meeting, Long Beach, California (2004)

4) J.Kouba: A Guide to Using International GPS Service (IGS) Products (Taken from IGS Website)

5) Y.E.Bar-Sever et al.: Estimating horizontal gradients of tropospheric path delay with a single

GPS receiver, JGR, **103**-B3, 5019/5035 (1998)
6) J.L.Davis et al.: Geodesy by radio interferometry: Effects of atmospheric modeling errors on estimates of baseline length, Radio Sciences, **20**-6, 1593/1607 (1985)
7) A.E.Niell: Global mapping functions for the atmosphere delay at radio wavelengths, JGR, **101**-82, 3227/3246 (1996)
8) G.Chen and T.A.Herring: Effects of Atmospheric Azimuthal Asymmetry on the Analysis of Space Geodetic Data, JGR, **102**-B9, 20489/20502 (1997)
9) D.D.McCarthy (ed.): IERS Conventions (1996), IERS Technical Note 21 (1996)
10) T.Tsujii et al.: Development of kinematic GPS software KINGS and its application to the observation of crustal deformations in the Izu-island district, J. Geod. Soc. Jpn,, **43**-2, 91/105 (1997) (in Japanese)

Masatoshi Honda (Non Member)
He received the B.S. degree from the Nihon University in 2001 and the M.E. from the Department of Aerospace Engineering at the National Defense Academy of Japan in 2007. He joined Maritime Self-Defense Force in 2001. Since April 2007, he has been with the Technical Research and Development Institute of the Ministry of Defense. His main research interests include applying estimation theory to the modeling and analysis of aerospace vehicles.

Masaaki Murata (Member)
He received the B.E. and M.E. degrees from Kyoto University in 1967 and 1969, respectively, and Ph.D. from The University of Texas at Austin in the Department of Aerospace Engineering in 1982. In 1969, he joined the National Aerospace Laboratory (now JAXA) and worked on satellite geodesy and GPS applications. Since 2003, he is a Professor in the Aerospace Engineering Department at the National Defense Academy of Japan. His research interests are in the area of applied estimation, satellite geodesy, precision orbit determination, and aerospace navigation. Currently he is developing GPS precise point positioning methods for aerial and space users. He is a member of the Geodetic Society of Japan and the American Astronautical Society.

Yukio Mizukura (Non Member)
He joined the National Defense Academy of Japan (NDA) in 1967. He received the B.S. degree from the Kantou Gakuin University in 1970. Since 1982, he is a Research Associate in the Department of Aerospace Engineering at NDA. His research interests include man machine system and human pilot of aerospace vehicles.